SUPPORTING INFORMATION

EXTENDED EXPERIMENTAL PROCEDURES

Luciferase Assay

Luciferase activity was assayed on muscle extracts by using a Luciferase Kit (Promega). Student's t-test was used to analyze statistical differences. Means ± SEM are shown. Differences were considered significant at $p<0.05$.

Real-time quantitative PCR and statistical analyses

For each point monitored, RNA extractions were performed on three pooled muscle samples or trypsinized cell culture. Total RNAs were extracted following the protocol provided with the RNAble reagent (Eurobio), from cultured cells or from pools of three muscles injected either with plasmids expressing GFP, GFP+OSK or non-injected (WT). More than four independent biological replicates were collected for each condition and at each time point tested. Concentration of total RNA was measured, and RNAs were stored in Tris 10 mM/EDTA 0.1 mM (pH7.4) at -80°C. To quantify mRNAs, 2 µg of total RNA was reverse-transcribed using High capacity cDNA Reverse Transcription kit (Applied Biosystems). Real-time Quantitative Polymerase Chain Reactions (real-time Q-PCR) were performed in technical duplicate for each sample on a 7300 Real-Time PCR System (Applied Biosystems) following manufacturer recommendations. Taqman Gene expression Assays (Applied Biosystems) were used for the mRNA detection of *mOct4* (Mm03053917_g1), *mSox2* (Mm03053810_s1) and *mKlf4* (Mm00492932_m1). For *Xenopus laevis* genes, real-time Q-PCR reactions were performed using Power SYBR® master mix (Applied Biosystems). Primers (MWG Biotech) were described in previous publications or designed using Primer Express Software (Applied Biosystems); the relevant sequences and references are listed in **Table S1**. Direct detection of the PCR product was monitored by measuring the increase in fluorescence generated by the TaqMan probe (*mOct4*, *mSox2*, *mKlf4*) or by the binding of SYBR Green to dsDNA (all others genes listed in **Table S1**). The threshold cycle (CT) of each target product was collected using 7300 system software (Applied Biosystem), and ΔCT between target and the DNA elongation factor type 1 α (*Ef1a*) as a loading control was calculated. The difference in ΔCT values of two groups (ΔΔCT) was used to calculate the fold-increase ($F=2^{-\Delta\Delta CT}$) and to determine the changes in target gene expression between conditions. Results are expressed as boxes representing minimum and maximum values around the median from an appropriate number of experiments as indicated in the figure legends. Non-parametric Mann-Whitney U-test was used to assess statistical differences in figures 4, 5, 6, S4 and S8; $p<0.05$ was considered significant (***: $p<0.001$; **: $p<0.01$; *: $p<0.05$; not significant (ns): $p>0.1$).

SUPPLEMENTARY REFERENCES

57. Cao, Y., Siegel, D., and Knochel, W. (2006) *Mech Dev* **123**, 614-625
58. Fini, J. B., Pallud-Mothre, S., Le Mevel, S., Palmier, K., Havens, C. M., Le Brun, M., Mataix, V., Lemkine, G. F., Demeneix, B. A., Turque, N., and Johnson, P. E. (2009) *Environ Sci Technol* **43**, 8895-8900
59. Xanthos, J. B., Kofron, M., Wylie, C., and Heasman, J. (2001) *Development* **128**, 167-180
60. Chang, C., and Hemmati-Brivanlou, A. (2000) *Mech Dev* **90**, 227-235
61. Ng, R. K., and Gurdon, J. B. (2008) *Nat Cell Biol* **10**, 102-109
62. Morrison, G. M., and Brickman, J. M. (2006) *Development* **133**, 2011-2022
63. Gao, H., Wu, B., Giese, R., and Zhu, Z. (2007) *Cell Res* **17**, 345-356
64. Le Grand, F., and Rudnicki, M. A. (2007) *Curr Opin Cell Biol* **19**, 628-633
65. Mochii, M., Taniguchi, Y., and Shikata, I. (2007) *Dev Growth Differ* **49**, 155-161
66. Chargé, S. B., and Rudnicki, M. A. (2004) *Physiol Rev* **84**, 209-238

SUPPORTING TABLE LEGEND

Table S1: Primer sequences used for real-time Q-PCR experiments. For each primer pair, the forward and reverse sequences are given; when relevant, the original publications are indicated and listed in Supplementary References.

Gene	Forward (F) & Reverse (R) primer sequences	Original reference
brg1	F: 5'-AGATGCACAAGCCAATGGATTC -3' R: 5'-CTCAGAGTTGCCCAGAGGT-3'	This paper
cerberus	F: 5'-AAGAGGAGCACGTAGGAGCAAG-3' R: 5'-GCCAAAATCACCATGCCC-3'	(57)
eef1a1	F: 5'-TGGATAGCCCCTGTGTTGGATT-3' R: 5'-TCCACGCACATTGGCTTTCCT-3'	(58)
gadd45a	F: 5'-CAACATCCTGAGAGTGAGCAACAT-3' R: 5'-AGAATACAATGCAGATCAGCAGTTT-3'	This paper
gata6	F: 5'-CCAACCGGGAGCCCCGATA-3' R: 5'-GCTGCTGTAGCCTGTATCC-3'	(59)
gdf3	F: 5'-CATGATGGAAGGTTTCGGAGTAC-3' R: 5'-TGGCTGCTATGGTTCCTTGAT-3'	This paper
hhex	F: 5'-AACAGCGCATCTAATGGGAC-3' R: 5'-CCTTTCCGCTTGTGCAGAGG-3'	(60)
myf5	F: 5'-TAGCTGTTCAGATGGCATGTCT-3' R: 5'-CGGAAGGGAGTCAGTGCTAC-3'	This paper
myoD	F: 5'-TACACTGACAGCCCCAATGA-3' R: 5'-TGCAGAGGAGAACAGGGACT-3'	(61)
myogenin	F: 5'-CCCAGCGGGTGGTATCAA-3' R: 5'-GTCATTCCATTCAGGGCTACAAG-3'	This paper
nr5a2	F: 5'-TGACCATTTCTTCGGCCATAC-3' R: 5'-GGCAGCGTGGTTTAGAGGTAG-3'	This paper
pax7	F: 5'-GGCCAAGCACAGTATTGACGGA-3' R: 5'-CCGGGTGTAAATGTCAGGATA-3'	This paper
sox17	F: 5'-GCAAGATGCTTGGCAAGTCG-3' R: 5'-GCTGAAGTTCTCTAGACACA-3'	(59)
xnot	F: 5'-CTGCATTTGGCCACCACCTGGC -3' R: 5'-GATGAGCCACACGGGTGGGTA-3'	(57)
xoct91	F: 5'-TAGTGATGGGCTGAGCAGTG-3' R: 5'-GGTGGTCTGGCTGAATGTTT-3'	(62)
xsox2	F: 5'-CCAGTCCACCTGTAGTCACCTCT-3' R: 5'-CACTTCTGCCCCAGGTAGGTAC-3'	(60)
xsox3	F: 5'-GGTTATGGTTTGGTCCCGGG-3' R: 5'-AGCGCCCAATCTTTTGCTG-3'	(57)
xtert	F: 5'-CGGTCTCCTTTCTTCAGCTATCA-3' R: 5'-CTCTTCTTTTCACAAACTCGTTGA-3'	This paper
xventx2	F: 5'-TTTCAGATGCTCTACCTGC-3' R: 5'-CAAATGGCCTTTCTTCCTG-3'	(63)

SUPPORTING FIGURE LEGENDS

Figure S1. Loss of reporter expression occurs for different concentrations of mouse OSK factors and different reporter constructs injected in tadpole muscle.
(***A***) Somatic transgenesis in tadpole tail muscles injected with CMV-GFP alone (GFP) or co-injected with the mouse OSK expression vectors (GFP+OSK), using 100 ng/µl (upper panel) or 400 ng/µl (lower panel) of each plasmid. A drop in GFP expression was observed in each condition, as for 200 ng/µl of each plasmid (see **Fig. 1**). Note that GFP decrease is less abrupt for 100 ng/µl condition, GFP-positive fibers being still numerous at 7 dpi and detectable at 14 dpi. Arrowheads indicate the same myomeric units at different time points. Kinetics analyses were repeated >3 times independently (n>10 for each time point) providing similar results. Scale bars: 500 µm. (***B***) Similarly, CMV-Luciferase (LUC) reporter expression showed a significant decrease in OSK-injected muscle, but not in controls (200 ng/µl of each plasmid), showing that this effect is not reporter-specific. (***C***) Using a SV40-LUC reporter construct produced similar results, showing that this effect is not promoter-specific. Luciferase quantifications were done at least twice (n≥10 in each group) and are expressed in % of the control in (***B***) or in Relative Light Unit (RLU) in (***C***). Means ± SEM are given, Student's t-test was used for statistical analysis: ***p<0.001; **p<0.01; *p<0.05; not significant (ns), p>0.1.

Figure S2. Cell clusters in OSK-transfected muscle have a nuclear organization that differs from apoptotic muscle.
(*A***) Multiple cell clusters (arrows) observed in an OSK-injected muscle at 7dpi. Each cluster is separated from the others by muscle fibers, suggesting independent origins. (***B*** and ***C***) Two examples of muscle fiber replacement in OSK-injected muscle at 7dpi. The overall shape of the cell clusters (arrowheads) fills a gap in the muscle fibers (f) organization, taking the place of disappeared (***B***; cl, cluster) or disappearing (***C***) fibers (see Figs. 1 and S1). (***D***) Nuclear disorganization seen throughout the whole OSK-transfected area at 14 dpi (myomeric units 2 to 5) contrasted with non-injected areas (myomeric units 1 and 6-7). (***E*** and ***F***) A clear difference was seen with the nuclear organization found in an apoptotic GFP-positive fiber, the nuclear material being more scattered along the apoptotic fiber and associated with bundle formations (arrows). Scale bars: 100 µm.

Figure S3. Cell clusters are obtained by injection of the mouse factors Oct4, Sox2 or Klf4 alone.
DAPI-staining was observed in transfected muscles at 14 dpi following injection of CMV-GFP and either CMV-Oct4 (***A***), CMV-Sox2 (***B***) or CMV-Klf4 (***C***), using 200 ng/µl per plasmid. Clusters surrounding the neighboring muscle fibers (*) were seen in each case, although less extended than those observed in OSK-injected muscles (see Fig. 3). As for OSK injection, clusters were labeled by alkaline phosphatase (***D-F***). At 14 dpi, weak cell proliferation (***G-I***) and numerous apoptotic cells (***J-L***) were observed in clusters using the PH3 and active Caspase-3 antibodies. These observations contrast with the situation seen in OSK-injected muscles (see **Fig. 3**). Scale bars: 100 µm. (***M***) Kinetics of cluster formation were compared between GFP-controls, OSK injection and the 3 factors injected separately (200 ng/µl for each plasmid). Except for GFP-controls, cell clusters were obtained in all conditions. For each point, 4≤n≤9 muscle samples were pooled from independent experiments, and the percentage of muscle with cluster was given.

Figure S4. Expression of exogenous mouse factors is lost in OSK-transfected muscle.
(***A***) Mouse *mOct4*, *mSox2* and *mKlf4* mRNA expression was monitored in OSK-transfected muscles using real-time Q-PCR. WT non-injected tadpoles served as controls, displaying no mouse transcripts (noted as Φ). Samples came from independent experiments, with 3 muscles pooled per sample (n≥4 per group) and mRNA levels are expressed as relative to OSK 3d. Q-PCR data are represented as described in **Fig. 3**. Significance was assessed *versus* the OSK 3d condition: **p<0.01; *p<0.05. Localization of the mouse factors in OSK-transfected muscles was observed at 7 dpi using specific antibodies against mouse Oct4 (***B***) and Klf4 (***F***) proteins, and the HA antibody that recognizes HA-tagged mOct4 and mSox2 (***C***). Separate injections of CMV-mOct4 (***D***) and CMV-mSox2 (***E***) showed that the two proteins are recognized by the HA antibody. Note that the 3 factors co-localized with the nuclei of GFP-transfected muscle fibers, but not with nuclei of neighboring cell clusters. (***G***) No co-localization of Pax7-positive satellite cells (arrowhead on magnification) and Oct4-labelled nuclei (arrows on magnification) was seen in OSK-transfected muscle observed at 1 dpi. Scale bar: 50 µm.

Figure S5. Myogenesis is reactivated during muscle repair in response to injection injury.
Expression of genes involved in myogenesis (64) was monitored at 3, 7, 14 and 21 dpi in GFP-controls (green boxes) and OSK-transfected muscles (red boxes), using real-time Q-PCR. For each gene, basal expression level in muscle of non-injected tadpoles is indicated (WT, black boxes). Myogenesis was reactivated in GFP-controls and OSK-injected muscles over 3 weeks, as previously reported for amphibian muscle regeneration (65). In both cases, *pax7, myf5* and *myogenin* mRNA levels increased, peaking at 14 dpi, returning at 21 dpi to levels similar to non-injected WT controls. The increase of *myf5* and *myogenin* expression was significantly higher for OSK at 7 dpi compared to GFP controls. *myoD* mRNA levels rapidly decreased at 3 and 7 dpi in GFP-controls and OSK-injected muscles, then transiently reappeared at 14 dpi, an increase related to myogenic differentiation of the neo-formed migratory myoblasts during the repair process (66). *myoD* expression dropped again at 21 dpi, probably with terminal differentiation in myofibers (66). Samples were from independent experiments, with 3 muscles pooled per sample ($4 \leq n \leq 8$ per group) and mRNA levels were expressed as relative to WT. Q-PCR data are represented as described in **Fig. 3**. Significance was assessed *versus* the WT condition, except when indicated by black bars: $**p<0.01$; $*p<0.05$.

Figure S6. OSK-reprogrammed cells maintain alkaline phosphatase activity in culture.
(***A***) Cell cultures were derived from GFP-controls or OSK-injected muscles at 7 or 12 dpi. After 1 day, 7 and 12 dpi OSK-derived cultures showed strong AP-positive colonies (***D*** and ***E***, respectively), whereas no labeling was seen in cultures derived from 7 and 12 dpi GFP-controls (***B*** and ***C***). Magnification of a 12 dpi OSK-derived colony displaying characteristic "ES-like" morphology (***F***) with strong AP activity (***G***) and high DAPI nuclear density (***H***). Scale bars: ***B-E***: 500 µm; ***F-H***: 10 µm.

Figure S7. Cultured OSK-reprogrammed cells differentiate spontaneously in various cell types.
Cell cultures were derived from OSK-injected muscles at 12 dpi, grown for 5 days in normal medium condition, and then alkaline phosphatase (AP) activity was revealed. (***A***) Small size colonies (arrow) with AP activity and compact ES-like morphology were still observable after 5 days of culture. (***B***) Two melanocyte-differentiated colonies showing no AP staining were easily identifiable by the presence of numerous characteristic pigmented cells. (***C-C'***) Neuronal differentiation was also observed for clones showing no AP labeling and characteristic axonal network: the same clone was observed after (***C***) and before AP staining (***C'***) to correctly distinguish axons. (***D-G***) Numerous differentiated OSK-derived colonies with varied cell morphology and showing no AP staining were also found after 5 days of culture. Scale bars: ***A-C*** and ***D-G***: 50 µm; ***C'***: 20 µm.

Figure S8. OSK-reprogrammed cells can differentiate into mesodermal and neurectodermal derivatives *in vitro.*
Differentiation through neurectodermal and mesodermal lineages was obtained following high Activin (100 ng/ml)+Noggin treatments of 12 dpi OSK-derived cultures, and revealed by real-time Q-PCR using specific markers (*xnot* and *myf5* for mesoderm and *sox2* for neurectoderm). After 3 days, spontaneous as well as induced differentiation was observed in non-treated (OSK) and treated (OSK+A) cultures but not in 12 dpi GFP-control derived cultures in similar conditions (GFP & GFP+A). Treatments were performed >6 times. Q-PCR data are represented as described in **Fig. 3** and mRNA levels expressed as relative to control cultures (GFP): $*p<0.05$; not significant (ns) $p>0.1$.

Supplemental Figure 1

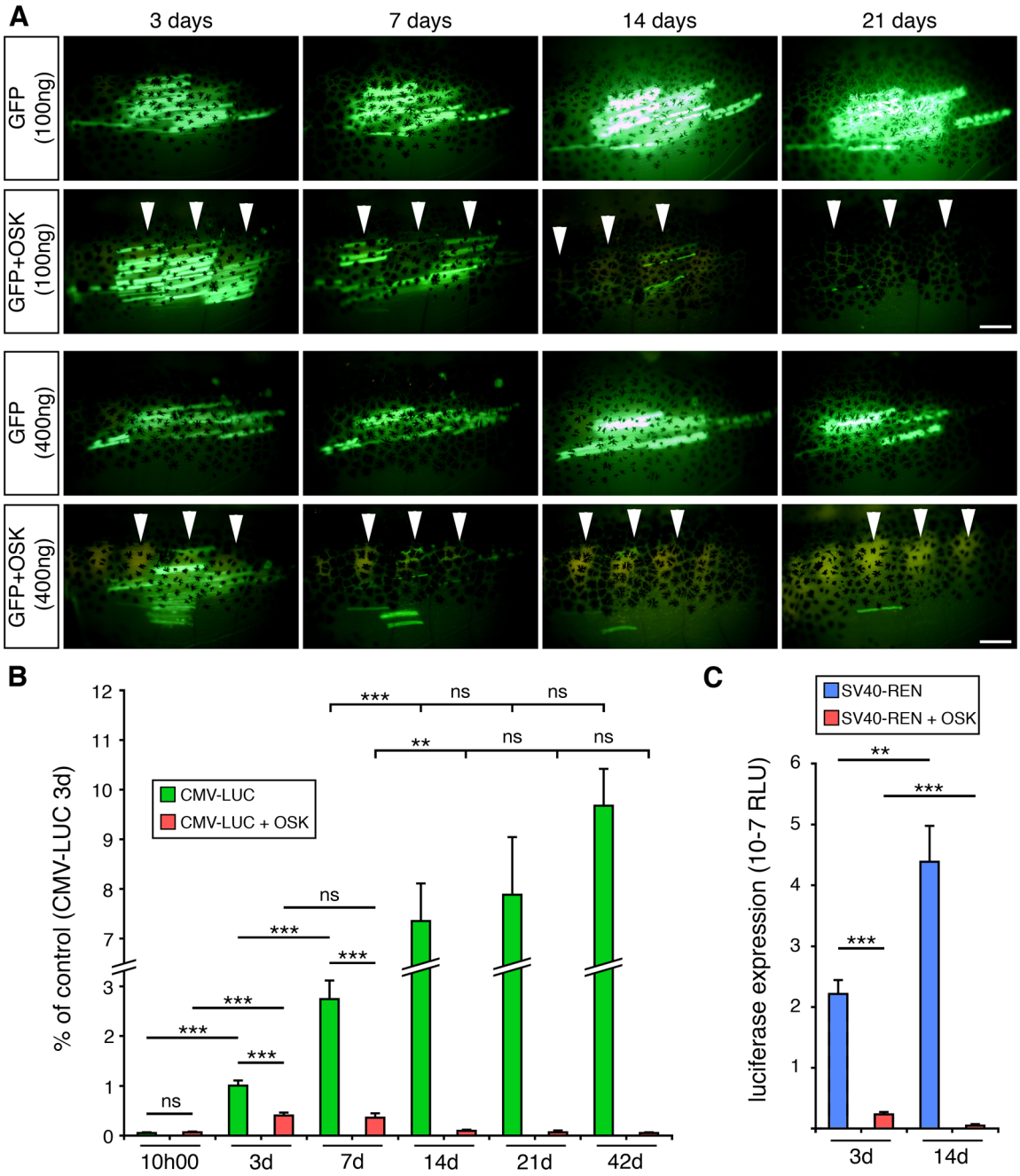

Supplemental Figure 2

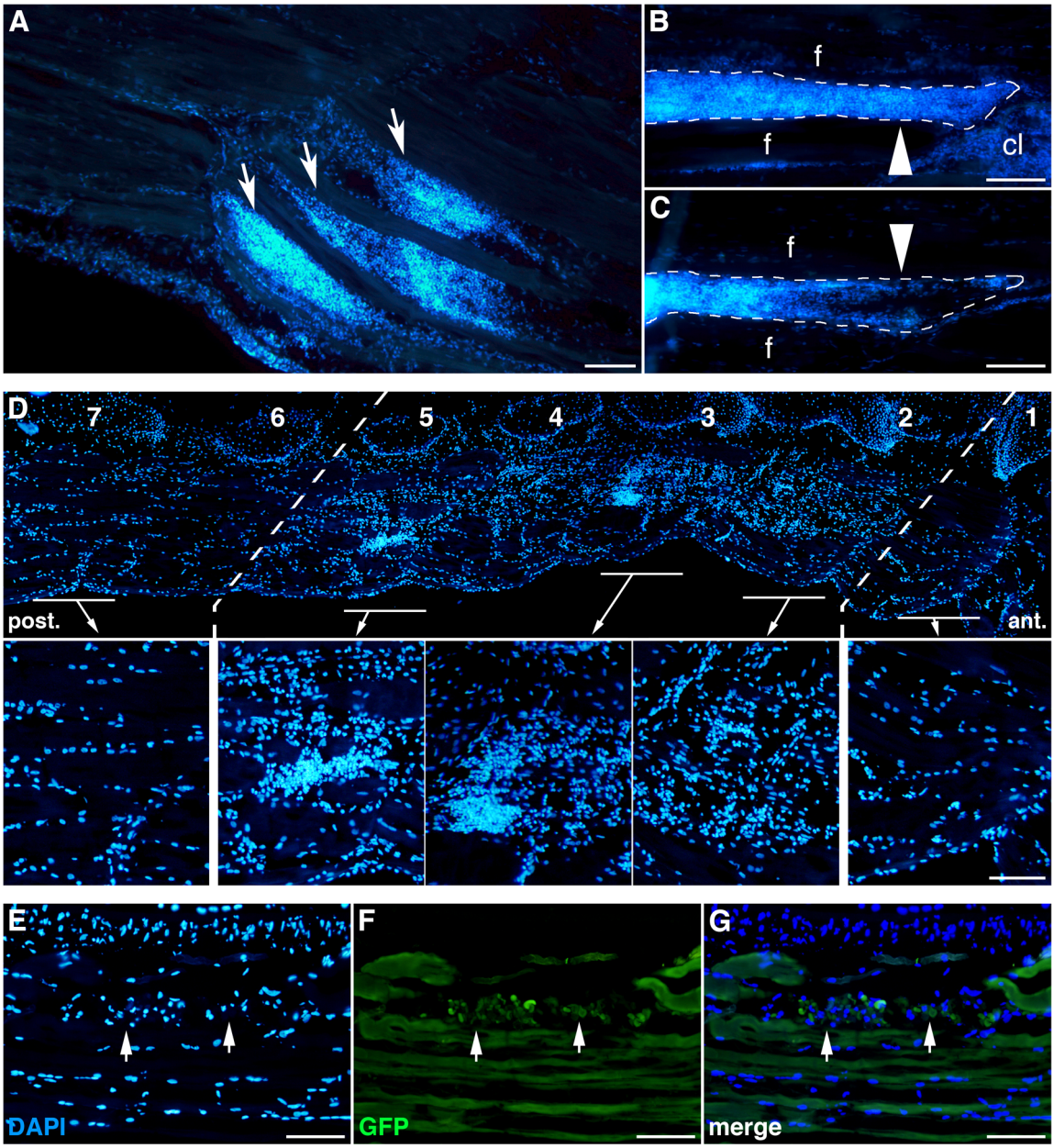

Supplemental Figure 3

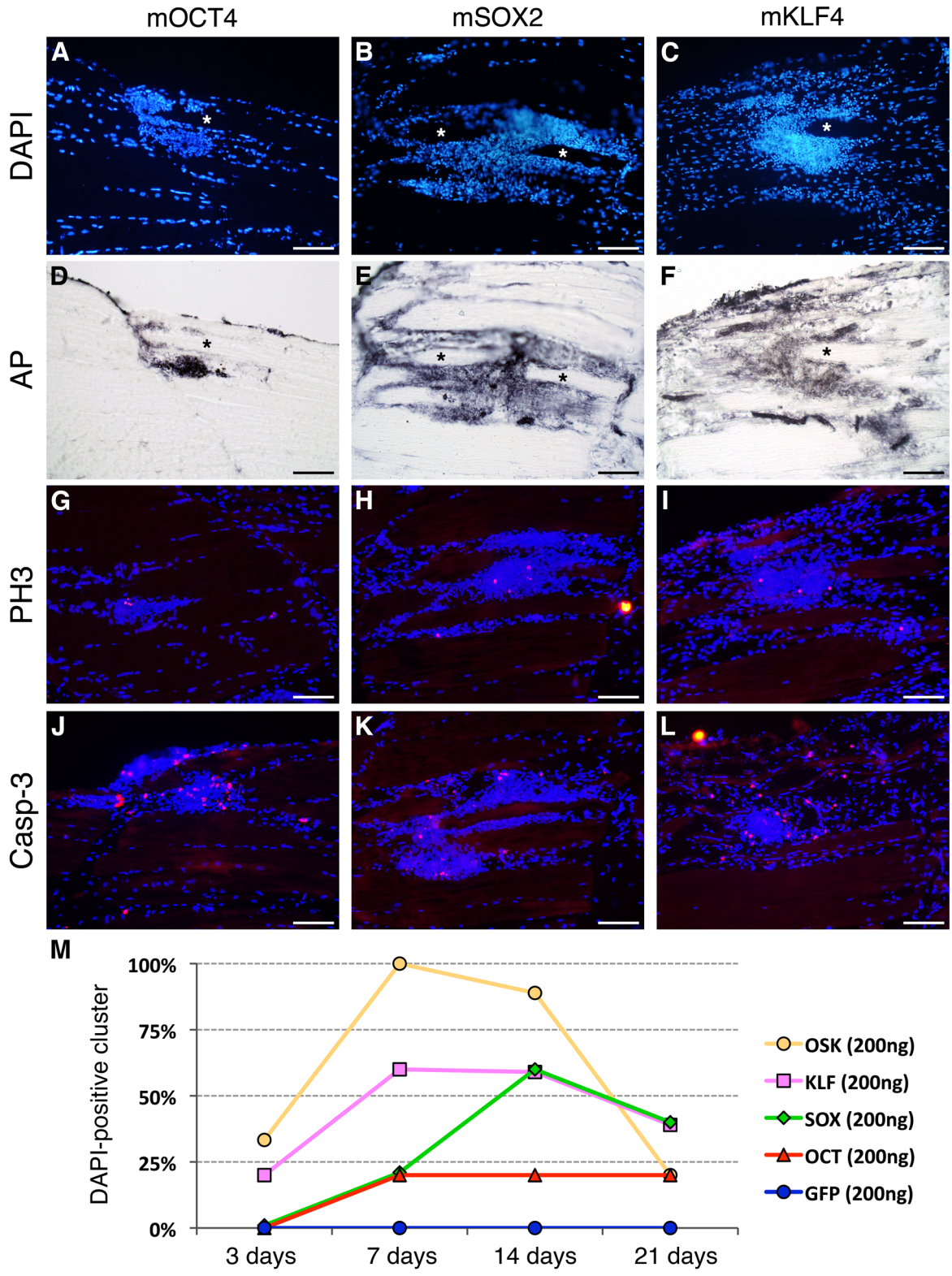

Supplemental Figure 4

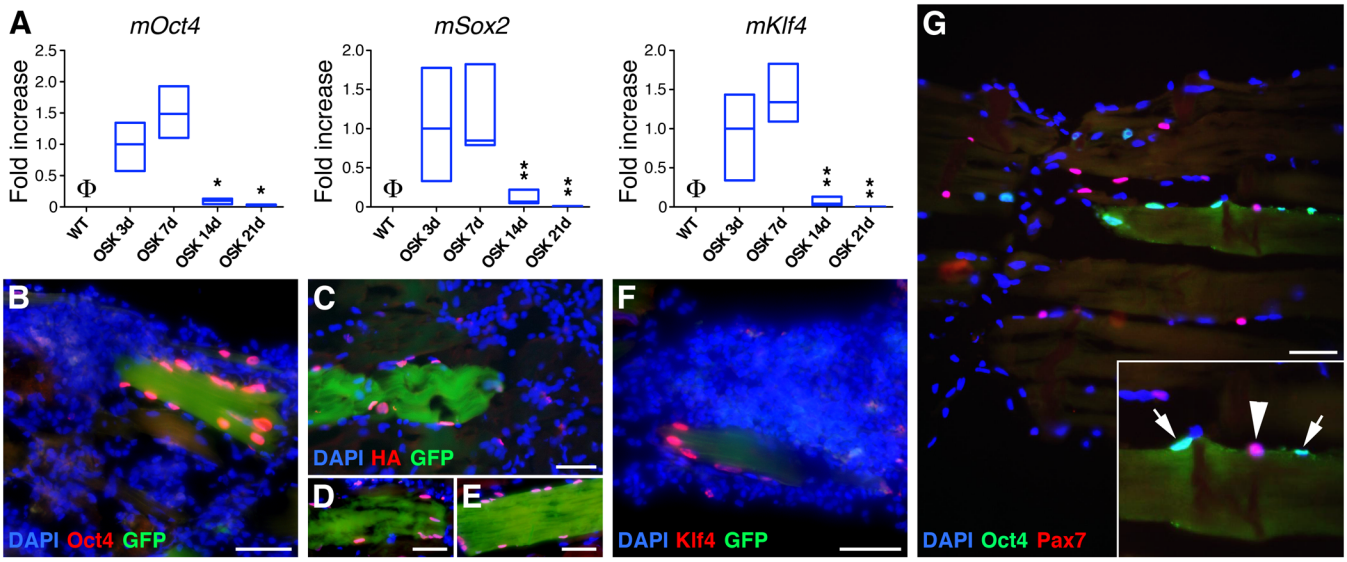

Supplemental Figure 5

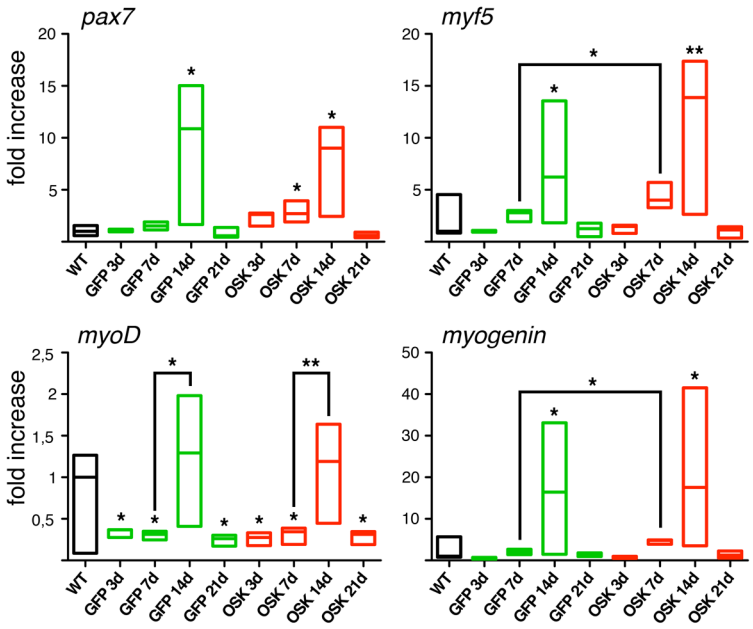

Supplemental Figure 6

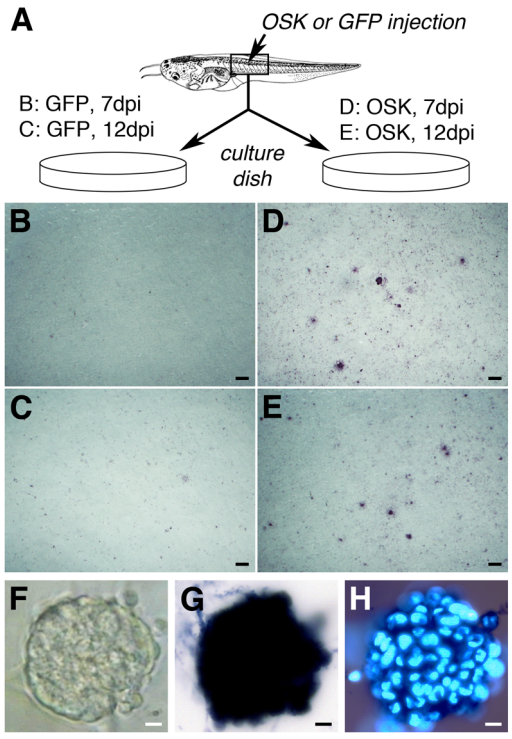

Supplemental Figure 7

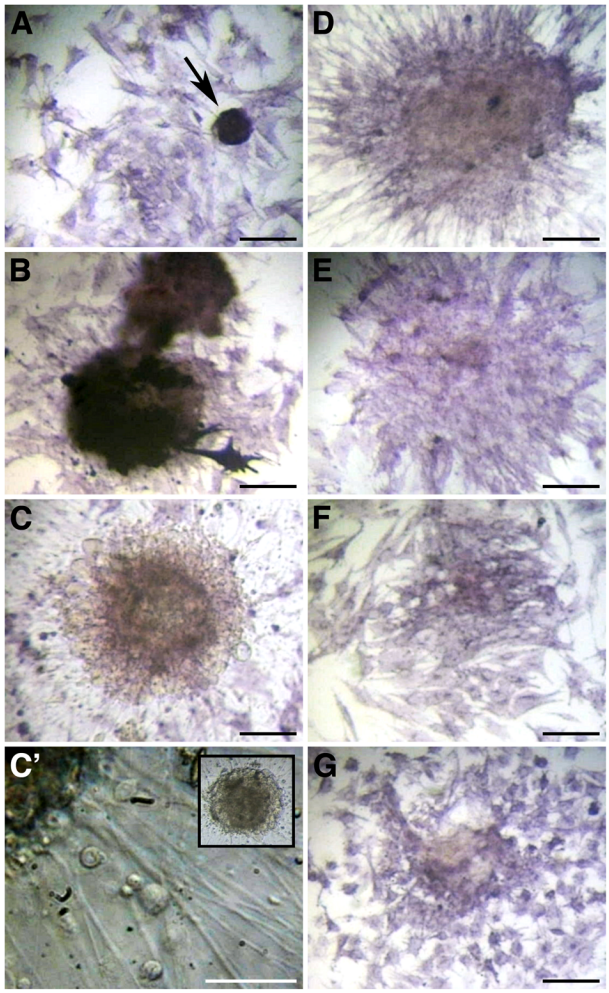

Supplemental Figure 8